Materials Research Express

PAPER • OPEN ACCESS

Investigation of the influence of carbon black on the rheology and electromechanical properties of ethylene butene copolymer

To cite this article: Yasin Hamid and Petr Svoboda 2020 *Mater. Res. Express* **7** 125303

Materials Research Express

OPEN ACCESS

RECEIVED
18 October 2020

REVISED
26 November 2020

ACCEPTED FOR PUBLICATION
8 December 2020

PUBLISHED
22 December 2020

PAPER

Investigation of the influence of carbon black on the rheology and electromechanical properties of ethylene butene copolymer

Yasin Hamid and Petr Svoboda

Department of Polymer Engineering, Faculty of Technology, Tomas Bata University in Zlin, Vavreckova 275, 762 72 Zlin, Czech Republic

E-mail: svoboda@utb.cz

Keywords: conductive polymer, ethylene-butene copolymer, dynamic mechanical analysis, carbon black, mechanical properties

Abstract

In this scientific article, the potential of producing a highly capable sensor by the addition of electric conductive carbon black (CB) to polymer composite was studied, and the effects of various carbon black content on ethylene-butene copolymer (EBC) on rheological and electromechanical were investigated. Electric conductive composites have many attempts at producing original material in technology as a sensor. The amount of (0, 4.07, 6.31, 8.71, and 11.28) volume % of CB was introduced to EBC using Brabender, mixed, and homogenized for 5 min at 180 °C. The dynamic mechanical analysis (DMA) and electromechanical test show that the addition of CB to the EBC would increase the viscosity, modulus, while electric resistance significantly decreased and changed greatly with elongation. The modulus increased from 8.9 to 15 MPa by increase of from 15 to 25 wt% of CB while the gauge factor decreases for about five times by increasing the CB from 15 to 25 wt% under 5 N force. These works demonstrate the possibility of producing strain sensors using a cheap and versatile technique, with potential health and electromechanical sensors.

1. Introduction

The fast development of smart sensors has contributed to smart elastic strain sensors. However, to date, the low stretch-ability and sensitivity of conventional metals or inorganic semiconductor-based strain sensors have restricted their application in this field to some extent [1–4]. Ethylene-butene copolymer (EBC), which is metallocene-based, is widely used in polymer modifications since it has excellent physical properties and is easy to process. EBC has been used with other polymers to increase the physical properties like tensile strength, rebound resilience, and compression set [5–8].

Carbon black (CB) is used as a filler and conductive particle in polymer materials. Several studies [9–13] have been done on CB filler rheological and linear viscosity with the composite's electrical resistance. It is relatively cheap and easy to use with excellent performance in its high electrical conductivity to its automotive, pressure sensor, and gas sensor [14, 15]. Thus, CB is the filler to reinforce the polymer blends to form a polymer composite. Instead, electrically conductive composites have been adequately prepared by adding an electrically conductive filler to polymeric materials. Several researchers have investigated the effect of the addition of various inorganic fillers such as carbon black, carbon nanotubes (CNTs) [16, 17], SiO_2 [18] Nanoclay [19] on the mechanical and electromechanical study of composites with conductive fillers. Slobodian *et al* [20] reported that the Spherical particles like Carbon Black in polymer/carbon black composites exhibit percolation threshold, frequently up to 15–25 wt.%. However, lower values were also published. D'Aloia *et al* [21] investigated that graphene's addition leads to an increase in the graphene-thermosets polymer's electromechanical and mechanical properties graphene concentration increase, the graphene-polymer composite undergoes an insulator-to-metal transition due to the presence of conductive filler inside the matrix. It is also reported that the addition of carbon nanotube to SEBS elastomer could increase electrical resistance. At the same time, the sample is stressed and decreasing when the sample recovers to initial deformation. Additionally, it has been shown that the sample leads to stable after some aging cycles [22]. Yang *et al* [23] investigated the resistance response of

CNT/graphene RTV silicone rubber composites under static and dynamic cyclic loading. It is observed that CNT/graphene RTV silicone rubber composites exhibited a stable and reproducible resistance response under dynamic cyclic loading, indicating that they have potential applications in continuous monitoring. It is also observed that the addition of Carbon nanotube could increase electric conductivity and increase the strain, leading to increased electrical conductivity [24]. Mostly, strain sensors are based on piezoresistive materials, for example, those materials for which an applied strain, ε, results in a resistance change. Commonly, the gauge factor is measured at low strain, which is most metals is small in the range 2 for Nichrome V to 4.8 for Platinum [25]. However, composite strain sensors based on polymers filled with conductive fillers, like multiwalled carbon nanotubes [26] and carbon nanotube [27, 28], can gauge high gauge factors. Piezoresistive materials resistance increases with increasing tensile strain as they have positive gauge factors because interparticle intersections dominate the piezoresistance in composites, leading absolutely to the Gauge factor higher than 0. A small number of materials with negative gauge factors [29]; polymer fibers coated with conducting polymers have demonstrated small negative gauge factors due to chain alignment effects.

Creep study of isotactic polypropylene (iPP)-based graphene nanocomposites used to evaluate the load transfer efficiency by Gaska [30] *et al* they have investigated that significant increase of Young's modulus with increasing filler content which indicates reasonably good dispersion and adhesion between isotactic polypropylene (iPP)-based graphene nanocomposites the and the filler content indicates reasonably good dispersion and adhesion between the iPP and the filler. Wang [31] *et al* reported the same results for numerical analysis using the Finite Element Method used for unidirectional fibrous polymer matrix composites' computing material properties. Srivatsan and Sreekanth [32] investigated the experimental characterization of dynamic mechanical properties of carbon fiber-reinforced composite with sandwich configuration. The addition of carbon fiber up to 40% wt will increase the loss modulus and tan delta curve as the frequency increases. They also indicated that Carbon exhibiting high storage modulus due to its atomic structure directly indicates young's modulus. Sabet *et al* [33] studied the impacts of graphene inclusion on the mechanical, electrical, and low-density polyethylene. They reported that while the addition of 3 wt% of graphene had a significant impact on the performance and improvement of LDPE's electrical characteristics, which is because of the spreading of graphenes in LDPE, which makes to extend more conductive networks. The polymer composite's viscosity is rasing from 120.1 to 195.4 kPa because of the significant interaction between the filler and matrix that obstructed the movement of macromolecular polymeric links. Consequently, graphene has an excessive surface area and nanoscale fat surface that renders it generate resilient interfacial connections with LDPE and significantly affects an excellent consequence of LDPE's chain movement.

The scope of this paper is to investigate the mechanical and electromechanical properties of conductive carbon black (CB) on ethylene Butene copolymer prepared with Brabender contain a various ratio of CB have been investigated. Both mechanical and electromechanical properties characterized by the composites were investigated experimentally. The effect on the piezoresistive response of the mixture was analyzed with an experimental strain-dependent measured electromechanical data. It is shown that the composites realized using a higher amount of CB show a higher electrical conductivity and a substantial increase in Young's Modulus.

2. Methodology

2.1. Material

Ethylene-butene copolymer (ENR 7467) was purchased from DOW Engage® chemical company in the USA with specific properties like ultimate tensile strength 2 MPa, tensile elongation of 600%. The melt flow index (MFI) is 1.2 dg min^{-1} and 0.862 g cm^{-3}. The conductive Carbon Black (KETJENBLACK EC300J) with the composition of 10 wt% polycarbonate with 99.95% purity is used for this study were purchased from Akzo Nobel Polymer Chemicals Ltd. Shanghai, PR China, with a bulk density of 0.125–0.145 g cm^{-3} and apparent density of 2.26 g cm^{-3}, pore volume (DBP) 310–345 ml/100 g and 3.9Ω·cm. This CB is mainly used as an electro-conductive filler used in resin compounds, electro-conductive battery materials, paint, colorant, and toner.

2.2. Preparation of composite

EBC/CF was prepared using Brabender, mixed, and homogenized with different concentrations (0, 10, 15, 20, 25 wt%) for 5 min at 180 °C at 60 rpm according to ASTM D7723 [34]. Then, compression molding was used to prepare the sheets with a thickness of 0.5 mm at 10 MPa with 5 min preheating and 6 min pressing at 180 °C. Finally, the dumble was prepared with a compression cutter for the test. The porosity density was measured according to Archimedes method ASTM B962–15 and was found to be less than 1% which is acceptable.

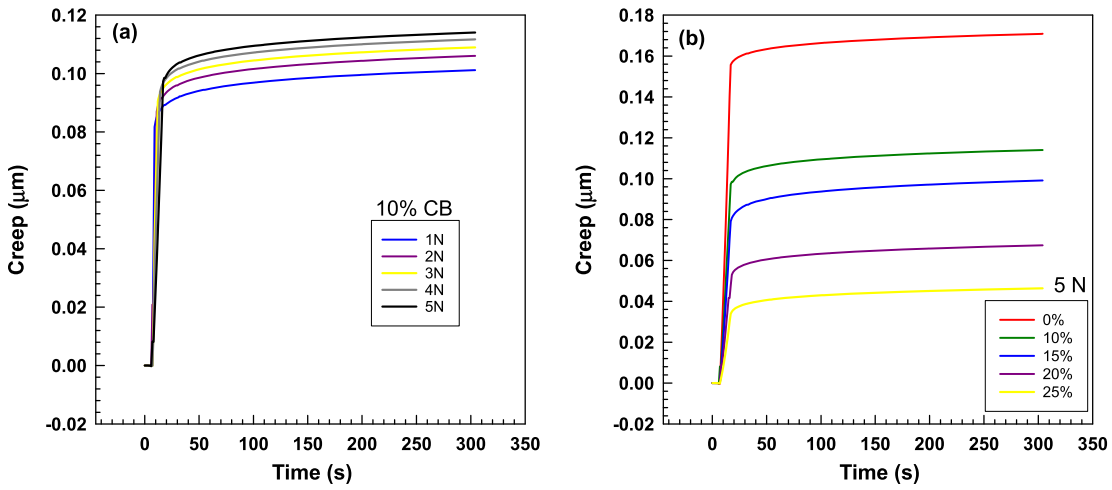

Figure 1. Creep–time for (a) 10% wt CB (b) 5 N curves of EBC/CB composite at 25 °C for different concentration and stress.

2.3. Electric resistance

The two-point probe method with a digital multimeter and four-point probe method using Hall Effect measurements is more common for electrical characterization. However, due to the limitation of four-probe measurement during the starching, the change in EBC/CB's electrical resistance change in strain-relaxation cycles was analyzed with precise weight using the two-point probe technique [35, 36]. Two single-terminal electrodes are attached to the surface of the conductive structure called the two-point probe technique. A DC or AC source current is then connected through the two electrodes, and the subsequent voltage over the same electrodes is estimated. The electrical resistance between these two electrodes is then determined, according to Ohm's law $I = V/R$ where I is the current through the conductor in units of amperes, V is the voltage measured across the conductor in units of volts, and R is the resistance of the conductor in units of ohms [37]. To increase the results' reliability, copper plates used as electrodes were attached to the sample, dissolved the backing adhesive, flooded into butanone solution, and then washed using tap water. After drying and cleaning copper plates, the pellets were sandwiched with upper and lower Ag's electrodes using silver paint around the surface of dumbbell specimens [38, 39]. The test was done using various forces (1, 2, 3, 4, 5 N) for 5 min to measure the strain and electric resistance change in time. When the samples are ready, an electrical circuit powered by a DC power source was applied to the DC source was used for the tests for its simplicity. Nonetheless, it is worth mentioning that, in reality, 1 kHz is commonly used to prevent polarization inaccuracy [37].

2.4. Dynamic mechanical analysis (DMA)

The dynamic mechanical analysis was calculated by the METTLER machine (Osaka, Japan). The samples with dimensions of $11 \times 11 \times 0.5$ mm were tested under Frequency sweep, stress-strain, and Creep relaxation. The stress-strain was analyzed by starting a force of 0 N to 5 N with a 0.5 N min^{-1} force rate at 25 °C. The creep relaxation was measured in three steps. At first, the sample was placed in the DMA machine for 1 min at 25 °C under 0.05 N. Then, the sample was under creep test for 5 min under 1 N force at 25 °C. This test was done for 1, 2, 3, 4, and 5 N respectfully, finally the force drops to 0.05 N for 5 min under 25 °C for relaxation. The frequency sweep test was done at 25 °C with a maximum force of 1 N between 0.1 to 100 Hz by ten steps per decade with 10 μm displacement. Higher frequency than 100 Hz is not recommended as all the specimen sizes except the one with 1 mm thickness are not useful due to their higher demand of displacement which the piezoelectric actuator is not capable of providing [40]

3. Results and discussion

The influence of Carbon black and force on shear stress, creep compliance, frequency sweep, and electromechanical study of the ethylene butene copolymer (EBC) was investigated by Dynamic Mechanical Analysis (DMA). Figure 1 indicates the effect of force and CB content on creep after 5 min of EBC/CB composite.

The creep of the composites with a content of 25 wt% of carbon fiber has the lowest value for almost four times compared to the pure EBC, which has the highest creep. Furthermore, increasing the force could increase

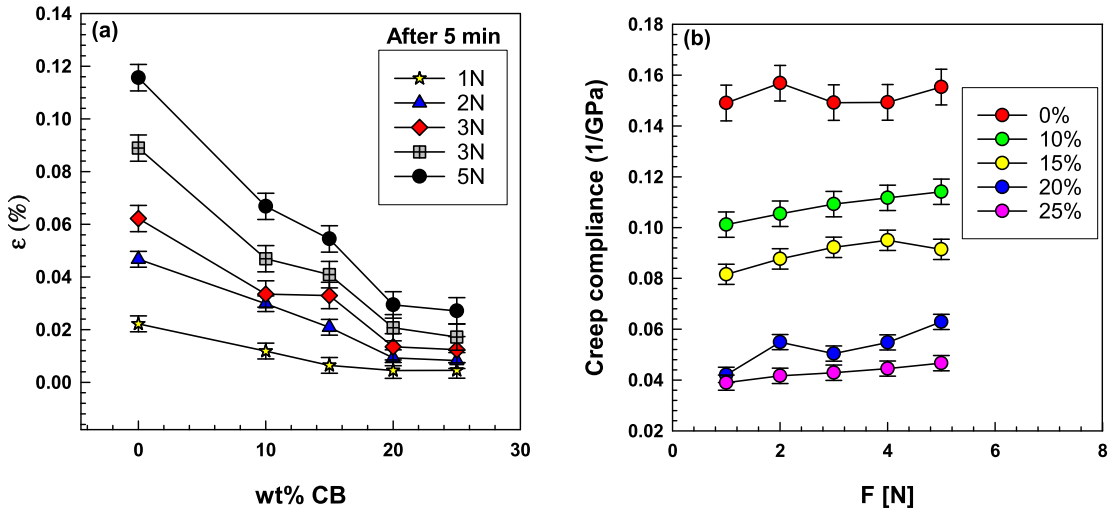

Figure 2. (a) Strain versus CB concentration for different force after 5 min (b) creep compliance versus force for different loading of CB content.

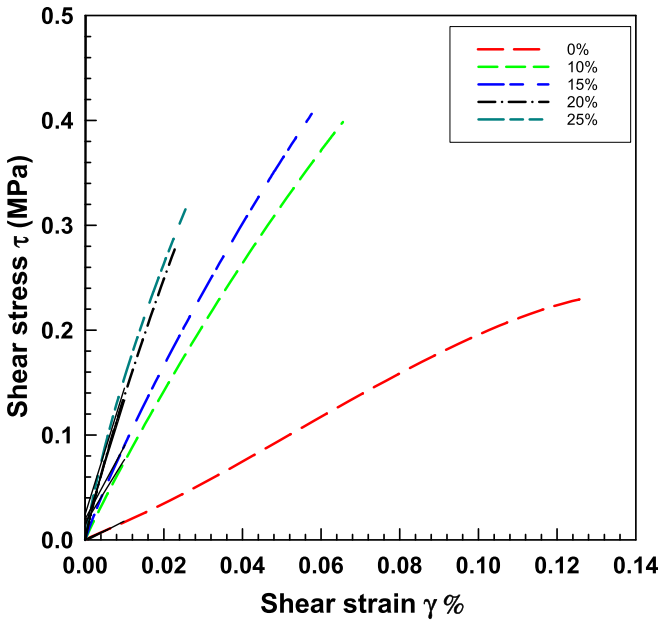

Figure 3. Representative tensile stress-strain curves for EBC/CB for different concentrations.

creep due to the improved interfacial action between the copolymer and the fiber [41]. Additionally, stiffness could be improved by fiber's addition by hindering the matrix material [42].

The stress and creep compliance was measured as a function of CB loading and forces in figure 2. It shows that elongation (ε) significantly decreased by increasing the CB content up to 20% wt. On the other hand, there is not much difference from 20% wt to 25% wt as the fiber looks well dispersed, and the filler covers the matrix. It also indicates that increasing the force up to 5 N could increase elongation six times due to the butene polymer composite's rubber behavior. The creep compliance graph shows that the addition of carbon black to the matrix decreases the creep compliance due to the significant interaction between the fiber and matrix, which leads to the increased modulus.

The Stress-strain tensile curves from DMA tests are shown in figure 3. It shows that the addition of CB to EBC would increase the modules Pa. Table 1 shows the modulus change by the addition of CB fiber at 0.01 shear strain [43] as mathematical representations rely on the linearity of response of both elastic and viscous components. It shows that by increasing the CB content to the matrix, the Young modulus would increase from 7.414 for 10 wt% Pa to 15.305 for 25 wt%. Savetlana *et al* reported that the addition of 20 wt%carbon black to the natural rubber could increase the modulus for 18 times from 2.5 to 47 MPa because of the reinforcing potential

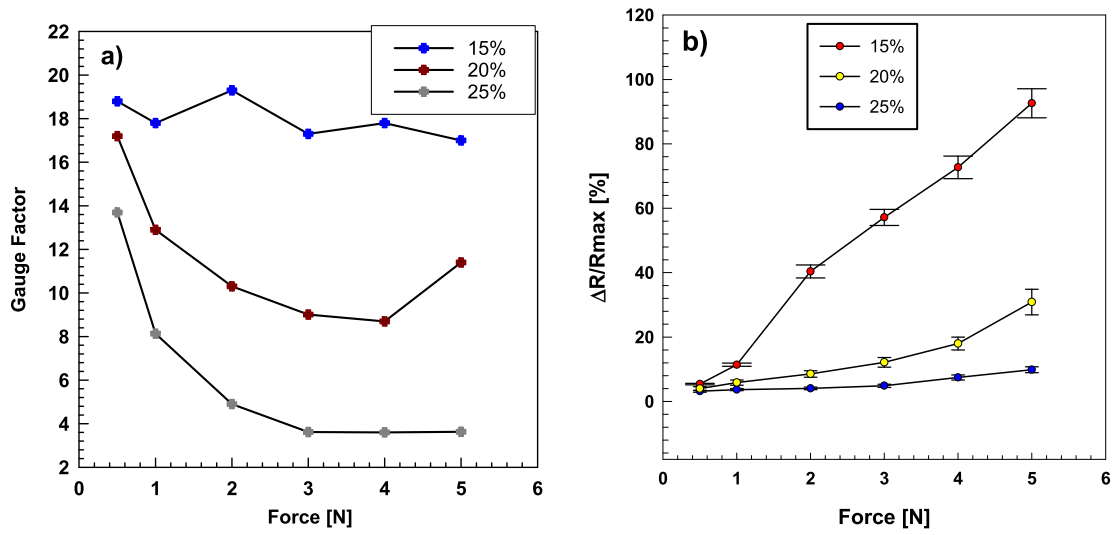

Figure 4. (A) Gauge factor (b) change of electrical resistance versus force for different concentrations of CB.

Table 1. Shear modulus G of EBC/CB composite at 0.01% shear strain.

CB content (wt.%)	Shear modulus G (MPa)
0	1.720 ± 0.08
10	7.414 ± 0.35
15	8.902 ± 0.38
20	13.670 ± 0.52
25	15.305 ± 0.71

from flexible filler formation network and strong polymer-filler coupling. The principal factors determined the capability of reinforcement were (i) Van der walls force between CB and polymer, (ii) the chemical cross-link of polymer into the filler surface due to the free radical reaction between carbon atoms in filler and polymer, and (ii) the mechanical interlocking of the polymer on to the filler surface [44]. Moreover, it looks like increasing fiber content. The copolymer composite tend to acts more brittle, which might be because of the quality of the fibers dispersion and good interaction between carbon black and ethylene butene copolymer. This is the global result of an efficient load transfer from the matrix to the first, strong chemical interactions and second, geometric interactions, such as the high specific surface area between the carbon black surface and the ethylene butane copolymer segments [45–47]. It has been established by numerous studies that addition of carbon base fibers exhibit a significant increase in modulus as compared to the matrix resin. As mentioned earlier, this is mainly due to the fact that functionalization improves both dispersion and stress transfer.

The electric resistance versus force is shown in figure 4(b). In this test, the electrical resistance was measured with a variety of loads for 5 min. However, the addition of CB up to 10% would not affect resistance. It might be related to the low concentration of carbon black in the matrix caused by disassociation between CB particles. That could decrease the resistance to almost zero. There are two types of electrical conduction in the EBC/CB: 'Contact' or 'tunneling' mechanism. Conductive fillers are physically in contact with each other and form a conducting network in the contact mechanism. Nevertheless, the electron's mobility has tunneled between the neighboring conductive fillers separated by the tunneling mechanism's polymeric layers [48, 49].

The gauge factor can be defined as [29, 50]

$$G = \frac{1}{\varepsilon}\left(\frac{\Delta R}{R_0}\right) \tag{1}$$

Where R_0 is initial resistance, ΔR is the change of resistance and ε is a strain. For a composite with strain-independent conductivity behavior, the following relationship is generally followed [51]:

$$\frac{\Delta R}{R_0} = \varepsilon(2 + \varepsilon) \tag{2}$$

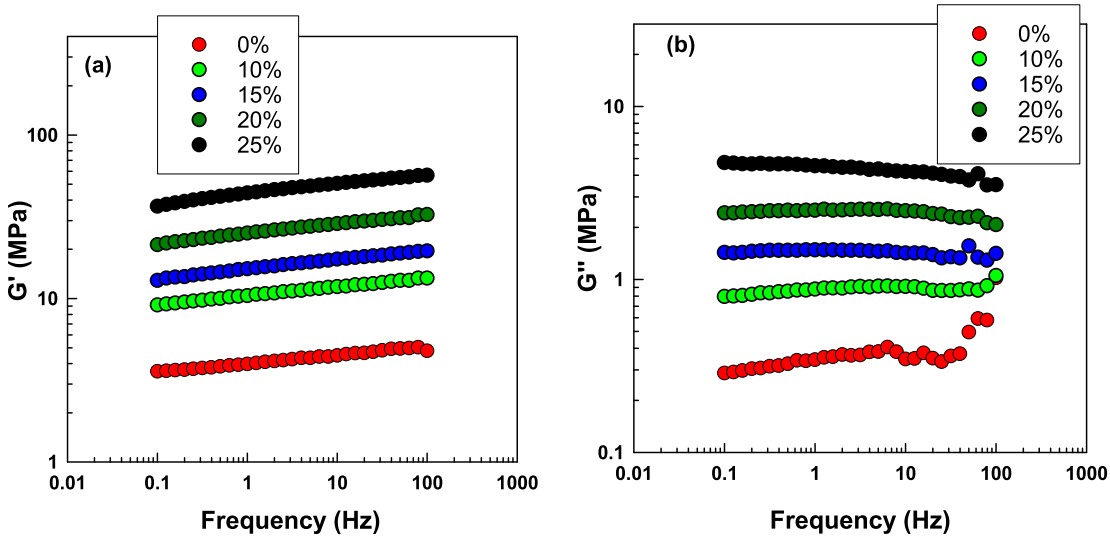

Figure 5. G′ (a), G″ (b), as a function of frequency composites for different CB content for EBC/CB.

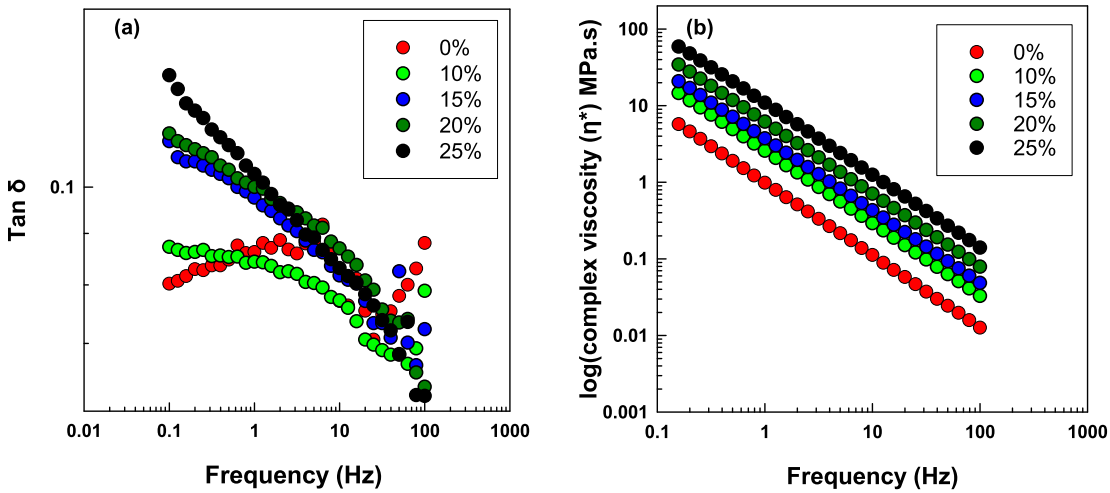

Figure 6. (a) tan δ (b) $|\eta^*|$ as a function of frequency composites for different CB content for EBC/CB.

Figure 4(a) indicates the gauge factor for different CB concentrations under force between 4 and 20, which is around five times higher than conventional metal gauge. It shows that the addition of CB to EBC could decrease the gauge factor with force. The gauge factor is around two at low strain, but it may be as high as 1300 for carbon nanotube/epoxy composite [52]. However, the most reported value is below 100 [50, 53, 54]. The addition of CB from 15 Wt% to 25 wt% leads to an increase in the resistance dramatically, increasing interaction and contacting the CB particles. Moreover, increasing the force leads to a decrease in the thickness of the sample. It caused an increase in the interaction of CB particles. Storage modulus (G') and loss modulus (G'') was tested as a function of shear strain (γ%). In the frequency sweep test, a small amplitude oscillatory shear, $\gamma^{\circ} = \gamma_o \sin(\omega t)$ was applied to the samples. Resulting shear stress was recorded as:

$$\sigma(t) = \gamma_0[G'(\omega)\sin(\omega t) + [G''(\omega)\cos(\omega t)] \quad (3)$$

G', G'' and dynamic viscosity (η^*) were measured as a function of angular frequency (ω) in the range of 0.1–100 rad s^{-1} at a strain value in the linear viscoelastic region [55, 56]. Figure 5 indicates the storage modulus (G′) and loss modulus (G′), Tan δ, and complex viscosity $|\eta^*|$ of the samples as a frequency function.

It is observed that the loose modulus (G′) is more sensitive than G′. It is well known that the storage modulus with the changes of CB content. There is no significant change in storage modulus observed for EBC/CB up to 20 percent because there is no interfacial interaction between CB fiber and EBC. However, EBC with 25% wt content will decrease the storage modulus up to 30% from 5 to 3.5 MPa for the entire frequency rate. On the other hand, it can be observed that G′ is increased significantly by increasing the frequency. It also can be

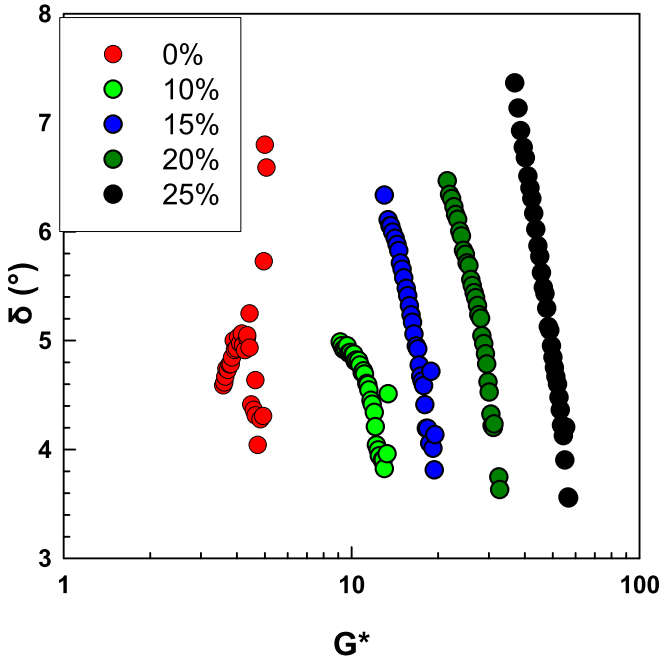

Figure 7. vGP of EBC for different CB content.

Table 2. Power-law factors determined from the $|\eta^*|$ versus log ω from figure 6(b).

ϕ% CB	Composite density g cm^{-3}	k	ω
0	0.862	−0.19512 ± 0.087	−0.94834
4.07	0.92	0.21998 ± 0.0103	−0.94573
6.31	0.95	0.382447 ± 0.0183	−0.94187
8.71	0.98	0.600717 ± 0.0284	−0.9416
11.28	1.02	0.84419 ± 0.0325	−0.93966

observed that the addition of CB up to 25% wt could increase G′ up to 3 times. Dependence of loss factor (tan δ) and complex viscosity $|\eta^*|$ of the samples on frequency is given in figure 6.

Tan δ curves of the polymer copolymer with CB decreased with increasing frequency. The negative slope in the Tan δ curve is a normal behavior of viscoelastic. In contrast, the positive slope refers to the elastic response of the viscoelastic samples dominating this elastic behavior.

$$\tan\ \delta = \frac{G''}{G'} \tag{4}$$

Figure 6(b). $|\eta^*|$ curves with frequency region were fitted by the power-law model to determine the shear-thinning phenomena. The dynamic viscosity is defined by [57]

$$\eta'' = \frac{G'}{\omega} \tag{5}$$

moreover, the elastic part of the complex viscosity:

$$\eta' = \frac{G''}{\omega} \tag{6}$$

$$|\eta^*| = (\eta'^2 + \eta''^2)^{\frac{1}{2}} \tag{7}$$

The power-law equation is written as:

$$|\eta^*| = \mathrm{k}\omega^n \tag{8}$$

Where $|\eta^*|$ is complex viscosity, k is a sample-specific pre-exponential factor, ω is the oscillation frequency in the frequency sweep test, and n is the shear-thinning exponent, which can be directly calculated from the logarithmic plot of complex viscosity $|\eta^*|$ versus frequency (ω) as

$$\log|\eta^*| = \log k + n\log(\omega) \tag{9}$$

The shear-thinning exponent, *n*, is the straight-line slope obtained by plotting $\log|\eta^*|$ versus $\log\omega$ [58–60].

Calculation of volume fraction (ϕ)

$$w_A = \frac{m_A}{m_A + m_B} \tag{10}$$

Furthermore, since:

$$V = \frac{m_A}{\varrho_A} \tag{11}$$

So

$$\phi = \frac{V_A}{V_A + V_B} \tag{12}$$

While the density of CB and EBC is 2.26 g cm^{-3} and 0.862 g cm^{-3}, respectively. The volume fraction is shown in table 2.

The van Gurp-Palmen (vGP) plot, which plots phase angle $\delta°$ versus complex modulus $|G^*|$, is sensitive to polydispersity and long-chain branching [61, 62].

The complex modulus $|G^*|$ is reported:

$$|G^*| = (G'^2 + G''^2)^{\frac{1}{2}} \tag{13}$$

As shown in figure 7, van Gurp-Palmen curves of EBC/CB show that the addition of CB to the EBC would increase. The blend shows the vGP plot predicted for linear polymers, i.e., a plateau at b = 7° in the low |G*| region.

The graphs show that additional CB content could increase $\delta°$ from 3.5° to 7°. Several studies have been reported about vGP, which have been similar tend peak followed by a downward tendency [62–65].

4. Conclusion

The linear viscosity and electromechanical properties of ethylene butene copolymers filled with electric conductive carbon black are investigated. The dynamic mechanical viscosity and modulus were found to be increased with the addition of carbon black into ethylene butene copolymer. Moreover, the electrical resistance is growing with carbon black content due to the interaction and contact between the particles. The elongation (ε) significantly decreases by increasing the CB content regarding the well disperses and hardening effect of CB. These work results establish manufacturing elastic strain sensors' potential using an economical and multipurpose method, with potential applications in flexible electronics products.

ORCID iDs

Yasin Hamid https://orcid.org/0000-0001-9786-6879
Petr Svoboda https://orcid.org/0000-0002-7320-5467

References

[1] Liu H, Li Q, Zhang S, Yin R, Liu X, He Y, Dai K, Shan C, Guo J and Liu C 2018 *Journal of Materials Chemistry C* **6** 12121
[2] Kim K-H, Hong S K, Ha S-H, Li L, Lee H W and Kim J-M 2020 *Materials Horizons* **7** 2662
[3] Akhtar I and Chang S-H 2020 *Nanoscale* **12** 21447–58
[4] Ke K, Sang Z and Manas-Zloczower I 2019 *Nanoscale Advances* **1** 2337
[5] Liu Z Y, Chen S J and Zhang J 2011 *J. Polym. Res.* **18** 2403
[6] Park K W, Chowdhury S R, Park C C and Kim G H 2007 *J. Appl. Polym. Sci.* **104** 3879
[7] Deng K Q, Felorzabihi N, Winnik M A, Jiang Z H, Yin Z H, Yaneff P V and Ryntz R A 2009 *Polym. Advan Technol.* **20** 235
[8] Escher F F N, Galland G B and Ferreira M R 2003 *J. Polym. Sci. Pol. Chem.* **41** 2531
[9] Wang Y K, Zhu G M, Cui X P, Liu T T, Liu Z and Wang K 2014 *Colloid Polym. Sci.* **292** 2311
[10] Oliveira F A, Alves N, Giacometti J A, Constantino C J L, Mattoso L H C, Man A M O A and Job A E 2007 *J. Appl. Polym. Sci.* **106** 1001
[11] Harea E, Datta S, Stenicka M and Stocek R 2019 *Express Polym. Lett.* **13** 1116
[12] Elhaouzi F, Mdarhri A, Brosseau C, El Aboudi I and Almaggoussi A 2019 *Polym. Bull.* **76** 2765
[13] Duan L, Spoerk M, Wieme T, Cornillie P, Xia H, Zhang J, Cardon L and D'Hooge D R 2019 *Compos. Sci. Technol.* **171** 78
[14] Gouma P I, Prasad A K and Iyer K K 2006 *Nanotechnology* **17** S48
[15] Biccai S, Boland C, O'Driscoll D *et al* 2019 *Acs Nano* **13** 6845–55
[16] Kumar Patel K, Purohit R, Hashmi S, Kumar Gupta R and Kumar Dwivedi S 2019 *Applied Innovative Research (AIR)* **1** 21–4 (http://nopr.niscair.res.in/handle/123456789/45842)
[17] Abidin M S Z, Herceg T, Greenhalgh E S, Shaffer M and Bismarck A 2019 *Compos. Sci. Technol.* **170** 85

[18] Qin J Q, Zhao H, Zhu R Q, Zhang X Y and Gu Y 2007 *J. Appl. Polym. Sci.* **104** 3530
[19] Islam M E, Mahdi T H, Hosur M V and Jeelani S 2015 *Procedia. Engineer* **105** 821
[20] Slobodian P, Lengálová A, Sáha P and Šlouf M 2007 *J. Reinf. Plast Comp.* **26** 1705
[21] D'Aloia A G, Proietti A, Bidsorkhi H C, Tamburrano A, De Bellis G, Marra F, Bregnocchi A and Sarto M S 2018 *Polymers* **10** 82
[22] Dios J R, García-Astrain C, Costa P, Viana J C and Lanceros-Méndez S 2019 *Materials* **12** 1405
[23] Yang H, Yao X F, Yuan L, Gong L H and Liu Y H 2019 *Nanoscale* **11** 578
[24] Slobodian P, Riha P and Olejnik R 2011 *New Developments and Applications in Sensing Technology* ed S. C. Mukhopadhyay, A Lay-Ekuakille and A Fuchs (Berlin: Springer) (https://doi.org/10.1007/978-3-642-17943-3_12)
[25] Fiorillo A, Critello C and Pullano S 2018 *Sens. Actuators, A* **281** 156
[26] Sanli A, Muller C, Kanoun O, Elibol C and Wagner M F X 2016 *Compos. Sci. Technol.* **122** 18
[27] Zhu Z H 2015 *IEEE Nanotechnol Mag.* **9** 11
[28] Ferreira A and Lanceros-Mendez S 2016 *Compos Part B-Eng.* **96** 242
[29] Biccai S, Boland C S, O'Driscoll D P, Harvey A, Gabbett C, O'Suilleabhain D R, Griffin A J, Li Z, Young R J and Coleman J N 2019 *ACS Nano* **13** 6845–55
[30] Gaska K, Manika G C, Gkourmpis T, Tranchida D, Gitsas A and Kádár R 2020 *Polymers* **12** 1309
[31] Wang Z and Smith D E 2019 *Compos. Struct.* **229** 111394
[32] Srivatsava M and Sreekanth P S R 2020 *Materials Today: Proceedings* **27** 931
[33] Sabet M, Soleimani H and Hosseini S 2020 *Polym. Bull.* **77** 459
[34] Thongnuanchan B, Nantayos W, Lopattananon N, Rattanapan S, Thitithammawong A and Nakason C 2019 *J. Polym. Environ.* **27** 1807
[35] Yee M J, Mubarak N M, Khalid M, Abdullah E C and Jagadish P 2018 *Scientific Reports* **8** 17295
[36] Tadesse M G, Mengistie D A, Loghin C, Chen Y, Wang L, Catalin D, Muller C and Nierstrasz V 2017 *17th World Textile Conf. Autex - Shaping the Future of Textiles*
[37] Ngabonziza Y and Li J 2011 *IMETI 2010-3rd International Multi-Conference on Engineering and Technological Innovation, Proceedings* 1, 241
[38] Huang Y, Li H and Qian S 2018 *Constr. Build. Mater.* **174** 253
[39] Sudakar C and Kutty T R N 2004 *J. Electron. Mater.* **33** 1280
[40] Esmaeeli R, Aliniagerdroudbari H, Hashemi S R, Jbr C and Farhad S 2019 *Modelling and Simulation in Engineering* **2019** 7026267
[41] Yu K J, Wang M L, Wu J Q, Qian K, Sun J and Lu X F 2016 *Nanomaterials* **6** 1–11
[42] Hamid Y, Abu Bakar A and Deirram N 2013 *J. Appl. Polym. Sci.* **128** 1170–5
[43] Capela C, Oliveira S and Ferreira J 2017 *Fibers Polym.* **18** 1200
[44] Savetlana S, Zulhendri, Sukmana I and Saputra F A 2017 *IOP Conf. Ser.: Mater. Sci. Eng.* **223** 1–9
[45] Hamid Y, Bakar A A and Deirram N 2013 *J. Appl. Polym. Sci.* **128** 1170
[46] Hamid Y, Svoboda P and Svobodova D 2020 *J. Vinyl Add. Tech.* **26** 325
[47] Le T-T 2020 *J. Compos. Mater.* **9** 1–25
[48] Varghese A M, Rangaraj V M, Mun S C, Macosko C W and Mittal V 2018 *Ind. Eng. Chem. Res.* **57** 7834
[49] Yousefi N, Sun X, Lin X, Shen X, Jia J, Zhang B, Tang B, Chan M and Kim J K 2014 *Adv. Mater.* **26** 5480
[50] Bhandari S 2019 *Carbon-Containing Polymer Composites* ed M Rahaman, D Khastgir and A K Aldalbahi (Singapore: Springer) (https://doi.org/10.1007/978-981-13-2688-2_14)
[51] Chen S, Lou Z, Chen D, Jiang K and Shen G 2016 *Adv Mater Technol-Us* **1** 1600136
[52] Anand S V and Mahapatra D R 2009 *Smart Mater. Struct.* **18** 045013
[53] Costa P, Oliveira J, Horta-Romarís L, Abad M-J, Moreira J A, Zapiráin I, Aguado M, Galván S and Lanceros-Mendez S 2018 *Compos. Sci. Technol.* **168** 353
[54] Zhou J and Hsieh Y-L 2018 *Acs Appl. Mater Inter* **10** 27902
[55] Adefisan O O and McDonald A G 2019 *Maderas. Ciencia y Tecnología* **21** 3–14
[56] Arulmurugan M, Prabu K, Rajamurugan G and Selvakumar A 2019 *Mater. Res. Express* **6** 1–13
[57] Macosko C W 1994 *Rheology - Principles, Measurements and Applications* (New York: John Wiley & Sons.)
[58] Durmuş A, Woo M, Kaşgöz A, Macosko C W and Tsapatsis M 2007 *Eur. Polym. J.* **43** 3737
[59] Durmus A, Kasgoz A and Macosko C W 2007 *Polymer* **48** 4492
[60] Mussatti F G and Macosko C W 1973 *Polymer Engineering & Science* **13** 236
[61] Gu L, Xu Y, Fahnhorst G W and Macosko C W 2017 *J. Rheol.* **61** 785
[62] Trinkle S, Walter P and Friedrich C 2002 *Rheol. Acta* **41** 103
[63] López-Barrón C and Macosko C 2014 *Journal of Rheology* **58** 1935–53
[64] Rulduà M L M, Raquez J, Re G, Santana O, Dubois P and Cailloux J 2019 *Materiales Compuestos* **3** 107–11
[65] Delgado D E, Sturdy L F, Burkhart C W and Shull K R 2019 *J. Polym. Sci., Part B: Polym. Phys* **57** 1246–54